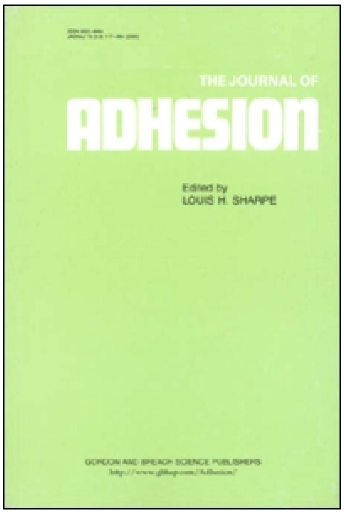

The Journal of Adhesion
Publication details, including instructions for authors and subscription information:
http://www.informaworld.com/smpp/title~content=t713453635

The Effects of Viscoelasticity in the Peeling of Polymeric Films

M. J. Loukis[a]; N. Aravas[a]
[a] Department of Mechanical Engineering and Applied Mechanics, University of Pennsylvania, Philadelphia, PA, U.S.A.

To cite this Article Loukis, M. J. and Aravas, N.(1991) 'The Effects of Viscoelasticity in the Peeling of Polymeric Films', The Journal of Adhesion, 35: 1, 7 — 22
To link to this Article: DOI: 10.1080/00218469108030432
URL: http://dx.doi.org/10.1080/00218469108030432

J. Adhesion, 1991, Vol. 35, pp. 7–22
Reprints available directly from the publisher
Photocopying permitted by license only

Printed in the United Kingdom

The Effects of Viscoelasticity in the Peeling of Polymeric Films

M. J. LOUKIS and N. ARAVAS

Department of Mechanical Engineering and Applied Mechanics, University of Pennsylvania, Philadelphia, PA 19104, U.S.A.

(Received November 5, 1990; in final form March 30, 1991)

A method to compute the interfacial fracture energy of a polymer film bonded to a rigid substrate, using the measured quantities of a peel test, is presented. The formulation is general and will accept any polymer which can be modeled as a linear viscoelastic material. The method is used to analyze the peeling of a polyimide film and a relationship between the fracture energy, the peel force, the speed of peeling and the thickness of the film is derived.

KEY WORDS Interfacial fracture energy; work of adhesion; polymer peeling; peel test; peel force; peel speed; film thickness; rigid substrate.

1. INTRODUCTION

The use of polymeric films by the microelectronics industry today continues to increase. These films are often bonded onto ceramic substrates and the interfacial strength of the bond is a very important design parameter. A mechanical test that is commonly used for the determination of the interfacial fracture energy is the so-called peel test, in which a film is peeled from a substrate. If the film deforms elastically during the test, then the peel force is a direct measure of the interfacial fracture energy; when the film deforms inelastically, however, the determination of the fracture energy is not as straightforward and peel test data must be used with great care.

There have been many elastic analyses of the peel test.[1–8] In most of these references, beginning with Spies[1] in 1953, the unattached part of the film is represented as an elastica while the attached film is modeled as an elastic beam on an elastic foundation. Meanwhile, there have been relatively few viscoelastic analyses to date. Chang[9] analyzed the peeling of an adhesive in terms of an elastic beam on a viscoelastic foundation and considered only the bonded portion of the film. Kendall[10] considered the peeling of a viscoelastic film from a rigid foundation and presented a very approximate solution to the problem. More recently, Aravas *et al.*[11] presented a general solution for the peeling of a standard three-parameter viscoelastic film from a rigid substrate.

A theoretical analysis to interpret peel test data of a polymer film is presented in this paper. The film is modeled as a linear viscoelastic material which is peeled away from a rigid substrate. A general methodology for the calculation of the interfacial fracture energy from the test parameters is given. The problem reduces to the solution of an integro-differential equation for the curvature of the film. Once the steady state distribution of curvature has been found, the corresponding viscous dissipation is easily determined, and the interfacial fracture energy is calculated by means of an energy balance.

2. GENERAL FORMULATION

2.1 Energy Balance

A schematic representation of the peel test is shown in Figure 1. A clear and concise way of determining the interfacial fracture energy of a bond in a bi-material system is through the use of an energy balance. The central feature in this approach is that it enables one to relate the *global energy* changes of the deforming film as a whole to the *local energy* requirement necessary to break the interfacial bonds and sustain crack growth or peeling. In this paper we will describe the mechanical behavior of the film in terms of a linear viscoelastic model.

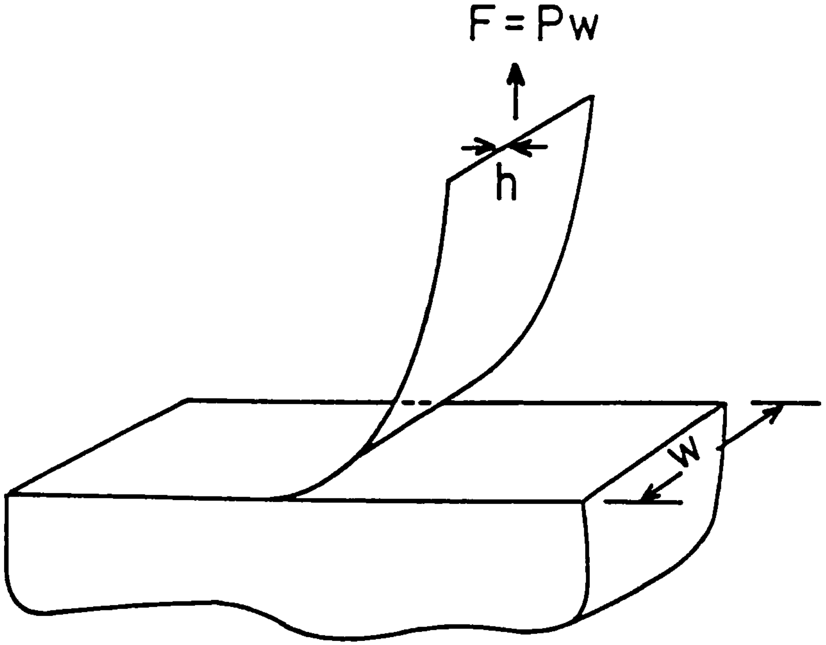

FIGURE 1 Schematic representation of the peel test.

If we consider an incremental crack advance during peeling, then the *external work* done by the peel force is balanced by the *elastic energy* stored in the film plus the *viscous energy* dissipated in the film while the remainder is expended in terms of the *separation work* required to break the interfacial bonds and create a new fracture surface. For *steady state* peeling, when the deformed shape of film remains the same as peeling proceeds, the energy balance can be written as

$$(1-\cos\phi)\,F\,dl = dW^e + dW^v + w\gamma\,dl, \tag{2.1.1}$$

where F is the peel force, ϕ is the peel angle (see Fig. 2), W^e is the elastic strain energy of the system, W^v is the viscous energy dissipation, γ is the adhesive fracture energy, w is the width of the film and dl is the virtual crack advance. Equation (2.1.1) can also be written as

$$\gamma = (1-\cos\phi)P - \psi_v - \chi, \tag{2.1.2}$$

where $P = F/w$ is the peel force per unit width,

$$\psi_v = \frac{1}{w}\frac{dW^v}{dl}, \tag{2.1.3}$$

is the viscous energy dissipated per unit width of the film per unit crack advance and

$$\chi = \frac{1}{w}\frac{dW^e}{dl}, \tag{2.1.4}$$

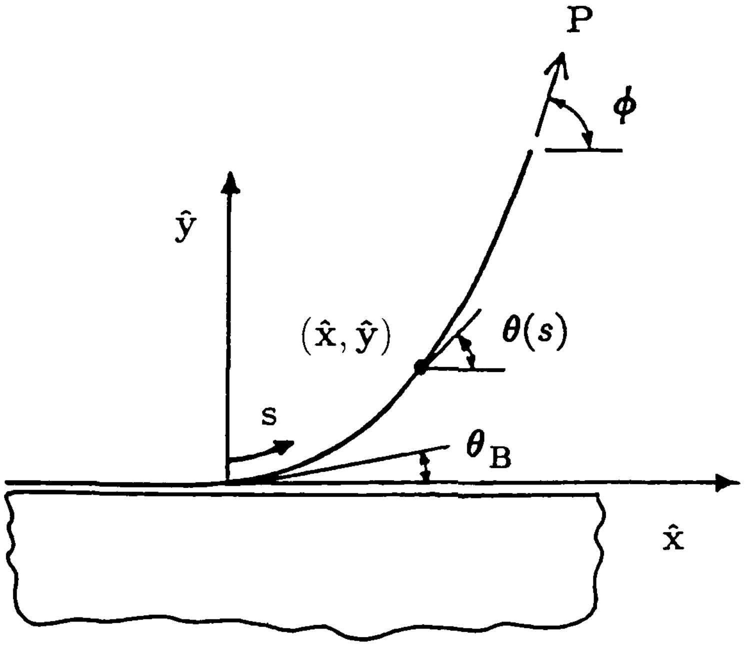

FIGURE 2 Schematic diagram of peeling.

is the elastic energy stored in the film per unit width of the film per unit crack advance.

During steady state peeling the shape of the deforming film remains constant and hence dW^e is due solely to the extension of the film. In most cases, the axial straining of the film is small compared with that due to bending; therefore, in the following, we assume that the film is inextensible so that $\chi = 0$. Equation (2.1.2) now reduces to

$$\gamma = (1 - \cos\phi)\, P - \psi_v\,. \tag{2.1.5}$$

The above equation shows very clearly that to compute the interfacial fracture energy γ, in addition to determining the peel force P from experiment, one must also compute ψ_v from an appropriate analytical or numerical technique. In the analysis which follows it will become apparent that once the steady state profile (or shape) of the unattached film has been obtained, the computation of the viscous energy dissipation ψ_v will be a straightforward exercise.

2.2 Governing Equations

The equilibrium equations of a slender beam undergoing *finite* deformation are

$$\frac{dT}{ds} - K(s)N(s) = 0, \tag{2.2.1}$$

$$\frac{dN}{ds} + K(s)T(s) = 0, \tag{2.2.2}$$

and

$$\frac{dM}{ds} + N(s) = 0, \tag{2.2.3}$$

where T and N are the axial and shear forces of the beam, $K = d\theta/ds$ is the curvature of the middle surface of the beam, $\tan\theta$ is the slope of the middle surface of the beam, M is the bending moment, and s is the arc length along the deforming film. Steady state peeling is assumed in the following.

Global equilibrium requires that

$$T(s) = Pw\cos(\phi - \theta(s)) \quad \text{and} \quad N(s) = Pw\sin(\phi - \theta(s)). \tag{2.2.4}$$

In the above equation $\tan\theta = d\hat{y}/d\hat{x}$, where $\hat{x}$-$\hat{y}$ is a cartesian coordinate system that translates with the moving crack tip, as shown in Figure 2. For definiteness, we also let $s = 0$ at the crack tip. The equilibrium equations (2.2.1) and (2.2.2) are now identically satisfied while the remaining moment equation (2.2.3) becomes

$$\frac{dM}{ds} + Pw\sin(\phi - \theta(s)) = 0. \tag{2.2.5}$$

A typical cross-section of the deforming film subject to a pure bending moment is shown in Figure 3. The sign convention and coordinate axes are as indicated such that a positive moment corresponds to a positive curvature. The width w is always

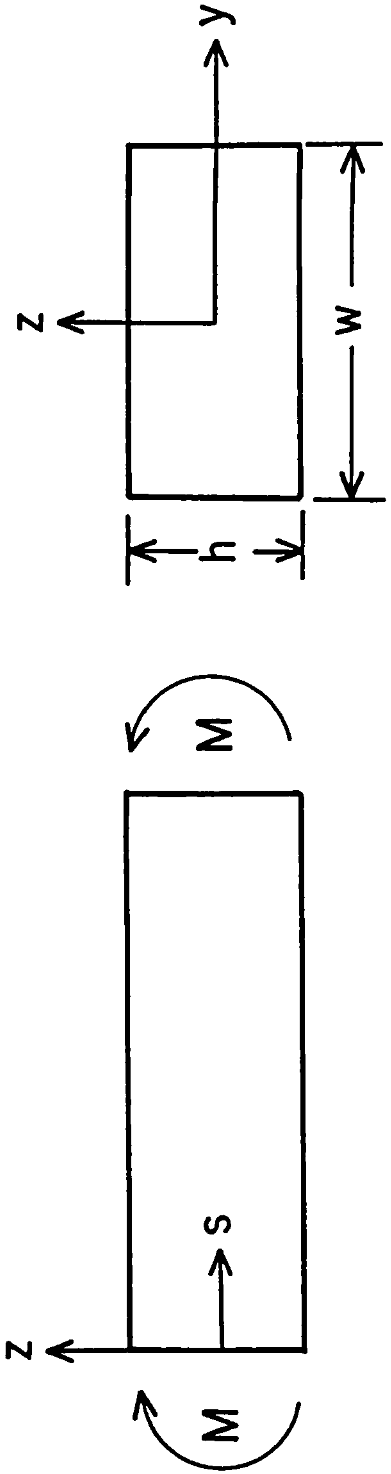

FIGURE 3 Beam under pure bending.

much larger than the thickness h and therefore plane strain assumptions are valid. If we assume that the film is inextensible and that plane sections remain plane and normal to the central axis, then the bending strain ϵ at any point along the film will be given by

$$\epsilon(s,z) = -K(s)z. \tag{2.2.6}$$

Here we assume that the deforming film experiences *small strains* and *large rotations*.

In this paper we will use the integral form of the constitutive equation for a linear viscoelastic material (*e.g.*, see Findley *et al.*[12]). During steady state peeling, the bending stress in the film is given by

$$\sigma(t,z) = \int_{-\infty}^{t} E\,(t-\tau)\,\frac{\partial\epsilon(\tau,z)}{\partial\tau}\,d\tau, \tag{2.2.7}$$

where σ is the stress, E is the viscoelastic stress relaxation modulus, t is the current time and τ is the time history from initial loading ($\tau = -\infty$) to the present ($\tau = t$). During steady state peeling of an inextensible film

$$s(t) = s_0 + vt, \tag{2.2.8}$$

will describe the distance, s, a representative material point will travel along the arc length of the film in time t from its original position of s_0 at $t = 0$. This same material point will travel a shorter distance

$$\xi(\tau) = s_0 + v\tau \tag{2.2.9}$$

along the film in time τ.

Substituting the time dependence of a material particle in terms of its spatial dependence we can, through the use of (2.2.9), write the constitutive equation as

$$\sigma(s,z) = \int_{-\infty}^{s} E\left(\frac{s-\xi}{v}\right)\frac{\partial\epsilon(\xi,z)}{\partial\xi}\,d\xi, \tag{2.2.10}$$

and by substituting for the strain in terms of the curvature, with (2.2.6), we find that

$$\sigma(s,z) = -z\int_{-\infty}^{s} E\left(\frac{s-\xi}{v}\right)\frac{dK}{d\xi}\,d\xi. \tag{2.2.11}$$

Finally, since the bending stress is related to the moment by

$$M(s) = -w\int_{-h/2}^{h/2} z\sigma(s,z)dz, \tag{2.2.12}$$

we may integrate equation (2.2.11) through the thickness, by using (2.2.12), to obtain

$$M(s)=I\int_{-\infty}^{s} E\left(\frac{s-\xi}{v}\right)\frac{dK}{d\xi}\,d\xi \tag{2.2.13}$$

where $I=\frac{1}{12}wh^3$ is the moment of inertia of the cross section.

In this paper, we consider the substrate to be *rigid* so that

$$K=0 \quad \text{for} \quad s<0, \tag{2.2.14}$$

and

$$K\neq 0 \quad \text{for} \quad s\geq 0, \tag{2.2.15}$$

where $s=0$ at the crack tip. Equation (2.2.13) can now be written as

$$M(s)=I\left[E\left(\frac{s}{v}\right)K(0)+\int_{0}^{s} E\left(\frac{s-\xi}{v}\right)\frac{dK}{d\xi}\,d\xi\right], \tag{2.2.16}$$

which is the moment-curvature relation for the unattached part of the film.

Finally, substituting (2.2.16) into the moment equilibrium equation (2.2.5) and using $K=d\theta/ds$ we arrive at the following integro-differential equation

$$\frac{d^2\theta}{ds^2}+\frac{Pw}{E(0)I}\sin\left(\phi-\theta(s)\right)+\frac{1}{E(0)v}E'\left(\frac{s}{v}\right)\frac{d\theta}{ds}\bigg|_0+\frac{1}{E(0)v}\int_{0}^{s} E'\left(\frac{s-\xi}{v}\right)\frac{d^2\theta}{d\xi^2}\,d\xi=0, \tag{2.2.17}$$

where prime denotes differentiation with respect to the corresponding argument, and the notation $A|_0$ is used to indicate the value of the function $A(l)$ at $l=0$. Equation (2.2.17) is the governing equation for $\theta(s)$ and the corresponding boundary conditions are

$$\theta=\theta_B \quad \text{at} \quad s=0, \tag{2.2.18}$$

$$\frac{d\theta}{ds}=0 \quad \text{at} \quad s=\infty, \tag{2.2.19}$$

where θ_B is the base angle which the film makes with the substrate at the crack tip (see Fig. 2).

Note that (2.2.17) is a general formulation for the peeling of any linear viscoelastic material, subject, of course, to the rigid base and inextensible film assumptions which have already been stated. Once $\theta(s)$ has been determined from the solution of (2.2.17), the profile $\hat{y}=\hat{y}(\hat{x})$ of the unattached part of the film can be determined from the integration of

$$\cos\theta(s)=\frac{d\hat{x}}{ds} \quad \text{and} \quad \sin\theta(s)=\frac{d\hat{y}}{ds}. \tag{2.2.20}$$

2.3 Viscous Dissipation

Once $\theta(s)$ is determined, the curvature is $K(s) = d\theta/ds$, and the corresponding moment distribution is given by (2.2.16). The viscous dissipation in the film per unit width w is given by

$$\psi_v = \frac{1}{w}\int_{-\infty}^{\infty} M(s)\frac{dK}{ds}\,ds = \frac{1}{w}\left[\frac{1}{2}M(0)K(0) + \int_{0}^{\infty} M(s)\frac{dK}{ds}\,ds\right], \qquad (2.3.1)$$

where $M(s)$ is determined by (2.2.16). Finally, the interfacial fracture energy is determined using equation (2.1.5).

3. EXAMPLE: POLYIMIDE PI 6015

3.1 Problem Formulation

In this section we will solve the integro-differential equation (2.2.17) subject to the boundary conditions (2.2.18) and (2.2.19) for Polyimide PI 6015, which is an acetylene-terminated polyimide manufactured by the National Starch and Chemical Corporation. Here we assume that the polyimide film contains no residual stresses prior to peeling.[15] The stress relaxation function for Polyimide PI 6015 has been determined experimentally[13] to be of the form

$$E(t) = \frac{E_1}{(t+t_0)^n}, \qquad (3.1.1)$$

where $E_1 = 4.1$ GPa·sec^n, $t_0 = 1$ sec and $n = 0.022$. Introducing the dimensionless quantities

$$\alpha = \frac{12Pt_0^n}{E_1 h}, \quad \beta = \frac{h}{vt_0}, \quad l = \frac{s}{h}, \quad \text{and} \quad \lambda = \frac{\xi}{h}, \qquad (3.1.2)$$

we find that the governing integro-differential equation (2.2.17) can be written as

$$\frac{d^2\theta}{dl^2} + \alpha\sin(\phi - \theta(l)) - \frac{n\beta}{(\beta l + 1)^{n+1}}\left.\frac{d\theta}{dl}\right|_0 - n\beta\int_0^l \frac{1}{[\beta\,(l-\lambda)+1]^{n+1}}\frac{d^2\theta}{d\lambda^2}\,d\lambda = 0. \qquad (3.1.3)$$

The corresponding boundary conditions are

$$\theta = \theta_B \quad \text{at} \quad l = 0, \qquad (3.1.4)$$

$$\frac{d\theta}{dl} = 0 \quad \text{at} \quad l = \infty. \qquad (3.1.5)$$

The α parameter contains the instantaneous elastic response in the film, whereas parameter β and the material property n represent the rate and stress relaxation effects, respectively, and are characteristic of the presence of viscosity in the film. Therefore, the first two terms in (3.1.3) are elastic terms while the third and fourth terms introduce the viscous effects. The moment-curvature relation (2.2.16) now becomes

$$m(l)=\frac{1}{\alpha}\left[k(l)-n\beta\int_0^l \frac{k(\lambda)d\lambda}{[\beta(l-\lambda)+1]^{n+1}}\right], \tag{3.1.6}$$

where

$$m(l)=\frac{M(s)}{Pwh} \quad \text{and} \quad k(l)=\frac{d\theta}{dl}=hK(s). \tag{3.1.7}$$

Equation (2.3.1) for the viscous energy dissipation can be now written as

$$\psi_v=P\left[\frac{1}{2\alpha}k_B^2+\int_0^\infty m(l)\frac{dk}{dl}dl\right], \tag{3.1.8}$$

where k_B is the dimensionless curvature at $s=0$.

The solution procedure for ψ_v is described as follows. We solve the boundary value problem consisting of the integro-differential equation (3.1.3), subject to the boundary conditions (3.1.4) and (3.1.5), for $\theta(l)$. The normalized curvature $k(l)$ and moment $m(l)$ are then determined from equations (3.1.7) and (3.1.6), respectively. Finally, with $m(l)$ and $k(l)$ determined at each point along the film, ψ_v can then be evaluated using (3.1.8).

3.2 Numerical Method

The integro-differential equation (3.1.3) is solved using a Galerkin- finite-element approach. The unknown function $\theta(l)$ is approximated by

$$\theta(l)=\sum_{j=1}^{N} w_j(l)\theta_j, \tag{3.2.1}$$

where $w_j(l)$ are the interpolation functions, N is the number of interpolating functions and θ_j are constants to be determined. The corresponding weighted residual statement is

$$\begin{aligned}\int_0^\infty w_i(l)\Bigg[\sum_{j=1}^{N}\frac{d^2w_j}{dl^2}\theta_j+\alpha\sin\left(\phi-\sum_{j=1}^{N}w_j(l)\,\theta_j\right)-\frac{n\beta}{(\beta l+1)^{n+1}}\sum_{j=1}^{N}\left.\frac{dw_j}{dl}\right|_0\theta_j,\\ -n\beta\int_0^l\frac{1}{[\beta(l-\lambda)+1]^{n+1}}\sum_{j=1}^{N}\frac{d^2w_j}{d\lambda^2}\theta_j d\lambda\Bigg]dl=0\end{aligned} \tag{3.2.2}$$

where $i=1,2,\ldots,N$. Equation (3.2.2) provides a set of N non-linear equations to be solved for θ_j, $j=1,2,\ldots,N$. Two-node isoparametric elements with two Gauss integration points are used in the computations and the resulting non-linear algebraic equations are solved using Newton's method. Two degrees of freedom per node are used, and the interpolation of θ within each element is defined by a third order polynomial in terms of the nodal values of θ and $d\theta/dl$. A total of 160 elements are used in the computations. The first 101 nodes are uniformly spaced at a distance $\Delta l = 0.5$ (or $\Delta s = h/2$) apart, while the spacing of the remaining 60 nodes increases by 10 percent for each succeeding node to a total length of approximately $l = 1700$ (or $s = 1700h$). Such a length is sufficient to model the region $0 \leq s < \infty$, since the unknown function $\theta(s)$ is found to vary extremely slowly with s for values of s greater than about $60h$. (See Figs. 4b and 5 below).

3.3 Numerical Results

In this section we present results for a peel angle of $\phi = 90°$ and a base angle $\theta_B = 0°$. The calculated angle $\theta(l)$ is plotted *versus* normalized arc length l in Fig. 4a, for $\alpha = 0.01$ and different values of the viscous parameter β, namely for $\beta = 0$, 1 and 10. It is readily noted that the curves $\theta(l)$ for $\beta \neq 0$ do not vary significantly from the curve representing the elastic solution $\beta = 0$, since the stress relaxation exponent is relatively small for this material ($n = 0.022$). Figure 4b gives the curve $\theta(l)$ for

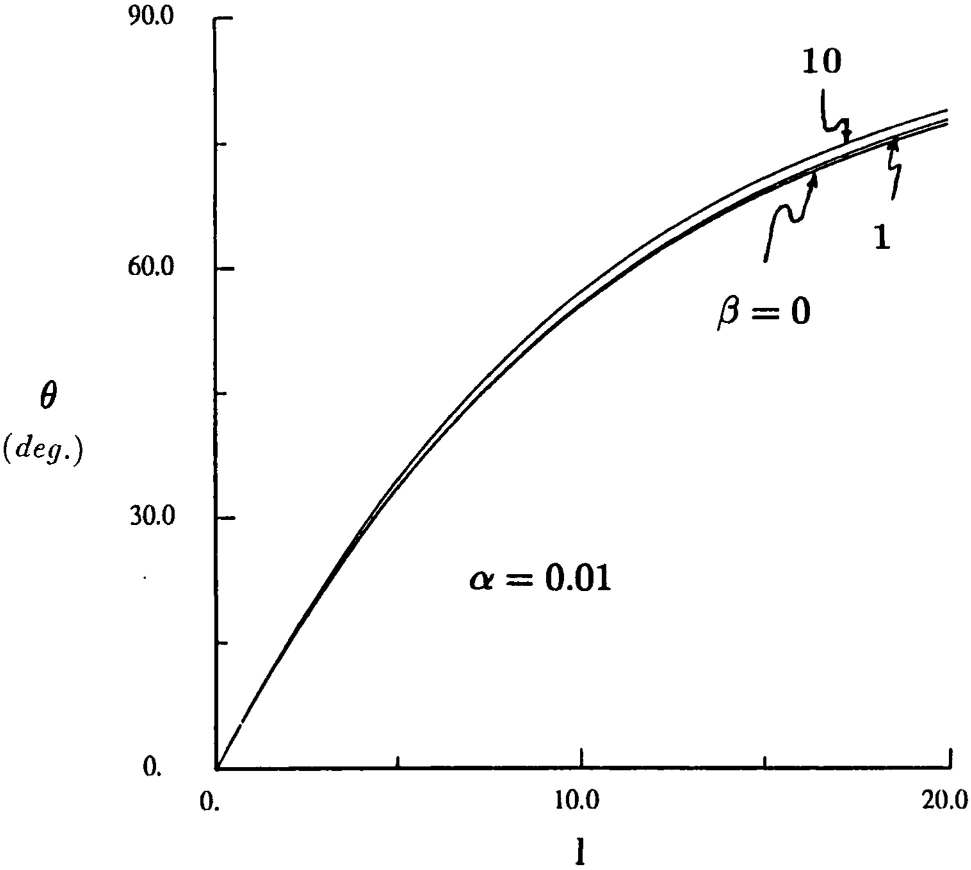

FIGURE 4a Peel angle θ *versus* arc length l for a given α and different values of β.

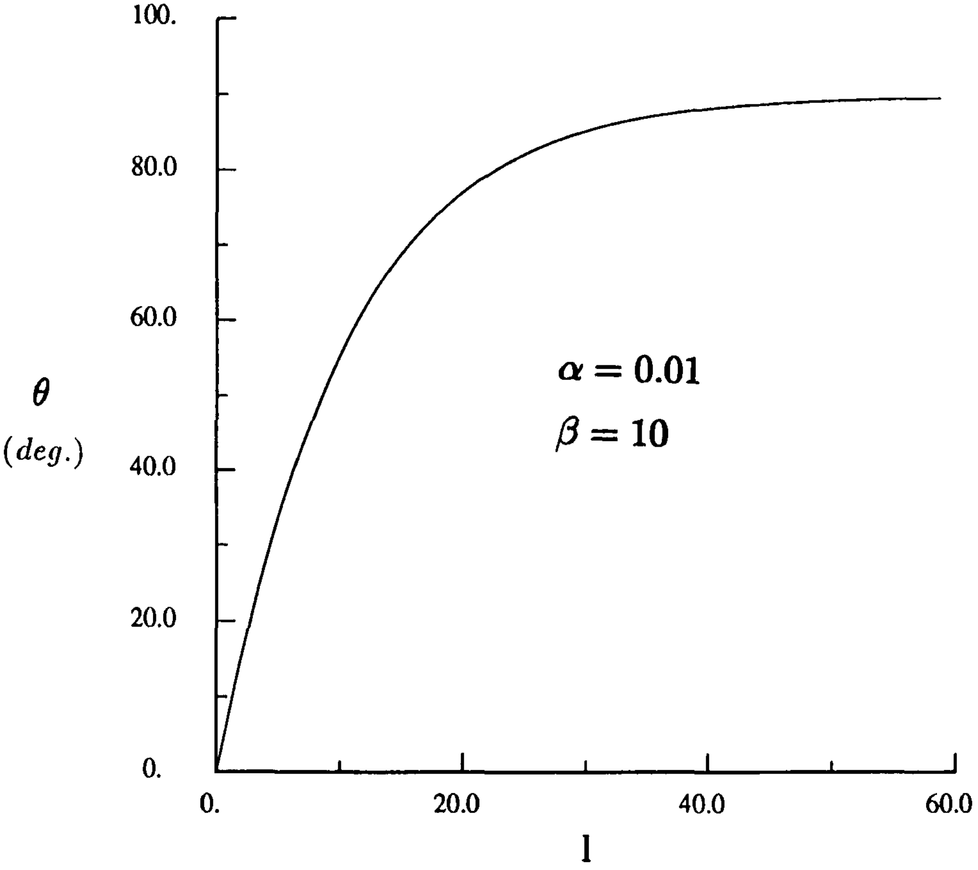

FIGURE 4b Peel angle θ *versus* arc length l for a given α and a given β.

$\alpha = 0.01$ and $\beta = 10$ and shows that when $l = 60.0$ then θ approaches the peel angle $\phi = 90°$.

The computed profile of the film is shown in Figure 5. It should be noted that the profile shown in Fig. 5 is not to scale, since the coordinate axes are scaled differently. Figure 5 shows that the curvature in the film increases as the viscous parameter β increases. Intuitively we find this to be correct since, as the modulus of the film relaxes in time, the bending stiffness (*i.e.* $E(t)I$) diminishes as well.

The moment-curvature history a material element experiences during steady state peeling is shown in Fig. 6. The straight line from A to B is indicative of the instantaneous elastic response of the film at the crack tip $s = 0$, whereupon the curvature of the film instantaneously jumps from zero to k_B, with a corresponding jump in the moment from zero to m_B. The curve below this line reflects the unloading behavior along the arc length of the unattached part of the film. The arrows indicate the directions in which loading and unloading proceed. The viscous energy dissipation ψ_v as computed by equation (3.1.8), is proportional to the area of the hysteresis loop in the moment-curvature diagram of Fig. 6.

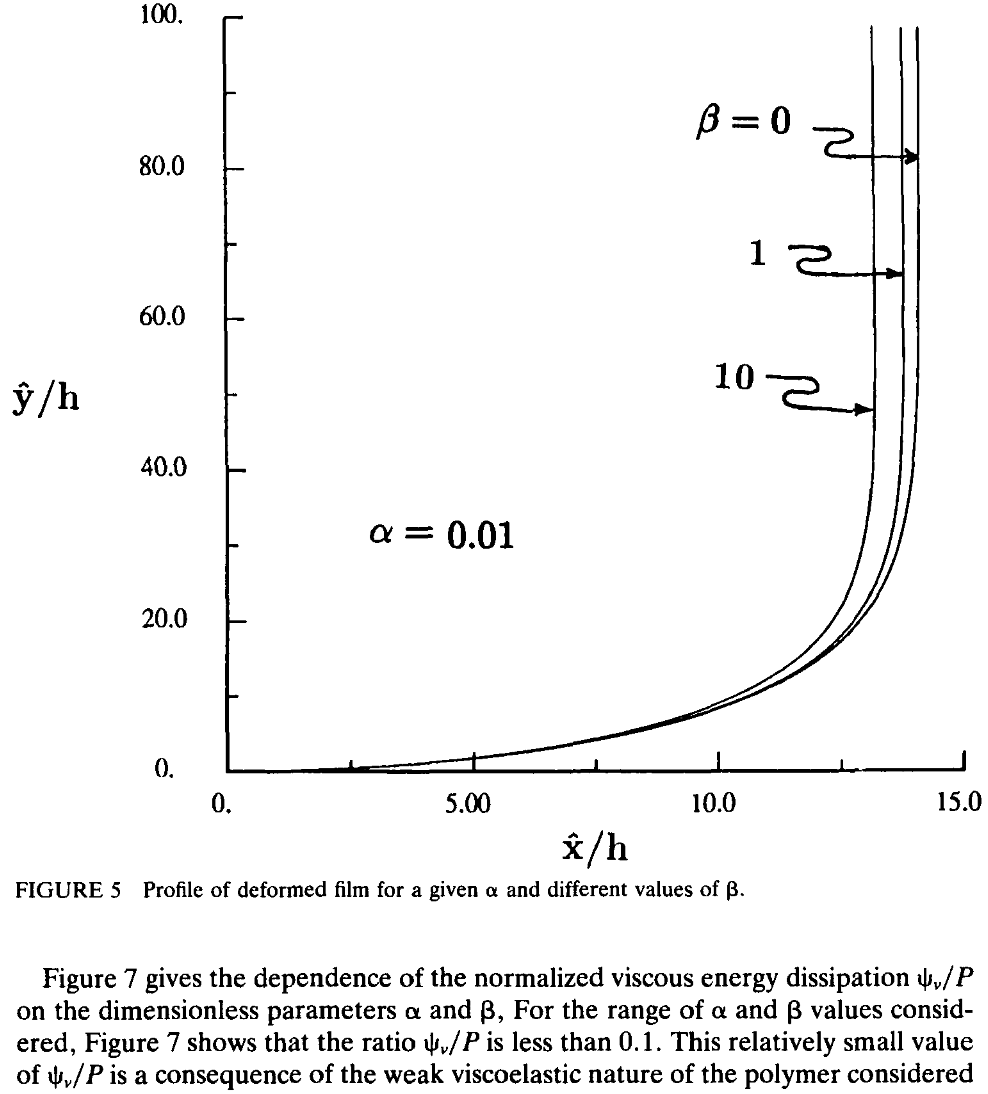

FIGURE 5 Profile of deformed film for a given α and different values of β.

Figure 7 gives the dependence of the normalized viscous energy dissipation ψ_v/P on the dimensionless parameters α and β, For the range of α and β values considered, Figure 7 shows that the ratio ψ_v/P is less than 0.1. This relatively small value of ψ_v/P is a consequence of the weak viscoelastic nature of the polymer considered ($n = 0.022$). It should be emphasized, however, that the value $\psi_v/P = 0.1$ should not be considered as a "typical" value for polymer peeling. In fact, in most cases, values much higher than 0.1 should be expected.

Furthermore, the ψ_v/P value calculated using the procedure outlined in Section 2 should be viewed as a lower bound to the actual ψ_v/P value, since the contribution of any axial strains to the energy dissipation is not included in our calculations. A discussion of the axial strain effects is given in the following section.

It is interesting to note the effect of film thickness h on the energy dissipation ψ_v. The parameter α varies like $\sim 1/h$ whereas β goes as $\sim h$; therefore, as the thickness of the film increases, α decreases, β increases, and as shown in Fig. 7, the ratio ψ_v/P will increase as well. It is worth noting that the opposite effect is observed in metallic films, where the ratio ψ/P decreases with increasing film thickness (Aravas *et al.*[11]).

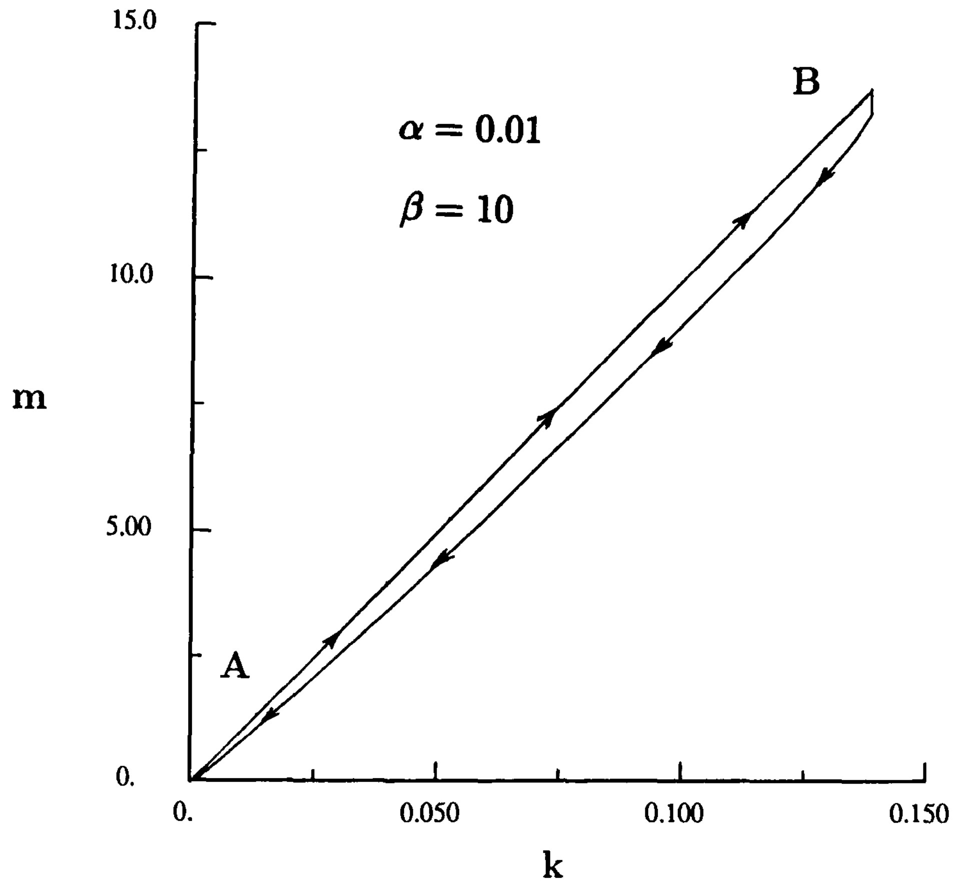

FIGURE 6 Normalized moment *m versus* normalized curvature *k* for a given α and β.

4. DISCUSSION AND CLOSURE

A detailed analysis of the mechanics of peeling of polymeric films has been presented. The primary aim of our work is to provide a theoretical basis for the proper calculation of the adhesive fracture energy γ from peel test data. Our analysis shows that the peel force alone is not sufficient for the determination of γ. Another important parameter which must be taken into account is the "base angle" θ_B, which depends on the properties of the film and the substrate, as well as on the adhesion strength itself. A method for the estimation of θ_B in a peel test has been presented by Kim[14] who modeled the attached part of the film as an elastic-plastic beam on an elastic (Winkler) foundation. A similar method could be used for a viscoelastic film. In such a model, however, the effects of the *singular* normal and shear stresses that develop along the interface in the region near the crack tip are neglected, and it is difficult to assess the accuracy of the calculated θ_B. We propose, instead, that θ_B be measured during the peel test. When the peel force P and base angle θ_B are

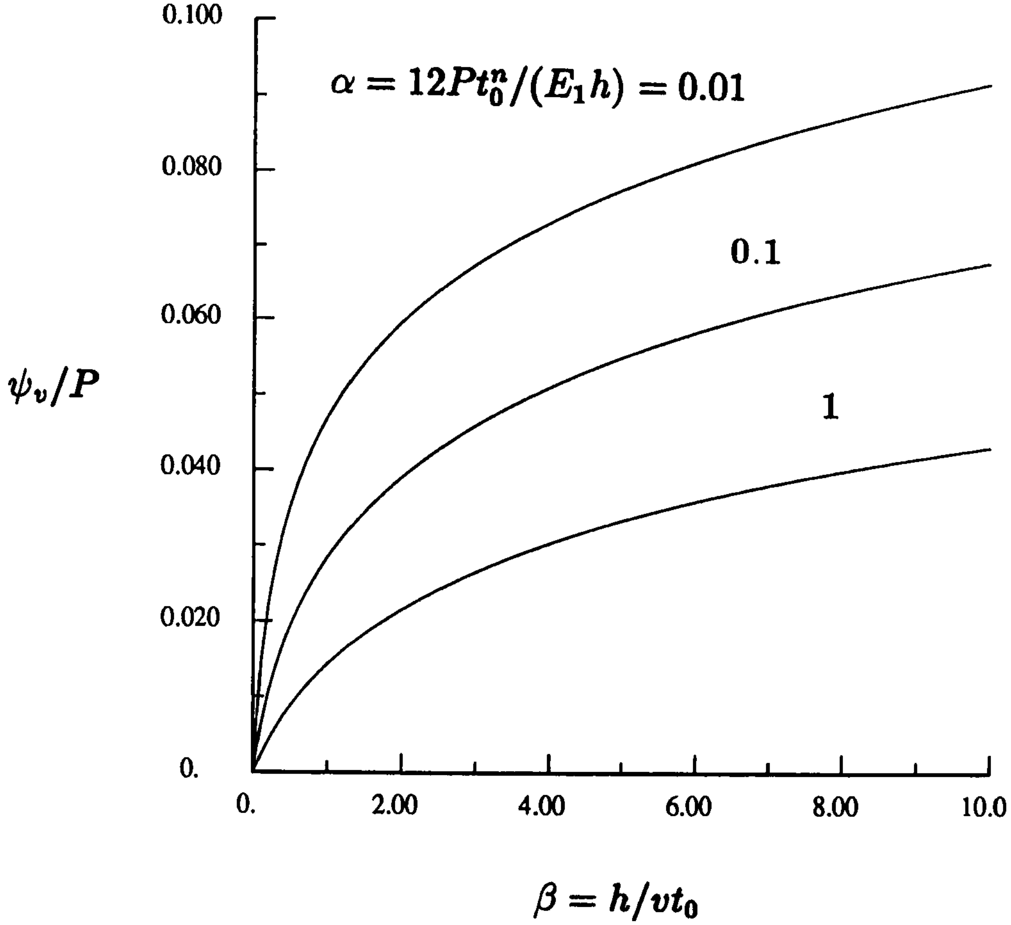

FIGURE 7 Normalized viscous dissipation ψ_v/P *versus* normalized viscous parameter β for different values of elastic parameter α.

known, the fracture energy γ can be calculated as follows. The energy dissipation ψ_v is determined first using Figure 7, and then fracture energy γ is found using equation (2.1.5), *i.e.*,

$$\gamma = (1-\cos\phi)P-\psi_v. \tag{4.1}$$

In that sense, Figure 7 is equivalent to the "universal peel diagram" developed by Kim[14] for metal films.

Several limitations of the present methodology are discussed in the following. Polymer films deposited on substrates are usually under substantial tensile residual stresses prior to peeling. The effects of those residual stresses are not accounted for in our formulation. It should be noted, however, that Loukis and Aravas[15] have recently shown that in metallic films, residual stresses smaller than 50% of the yield stress of the metal have a very small effect on the energy dissipation during a peel test. Therefore, as a first approximation, one could argue that in polymer films such effects can also be ignored as long as the residual stress is smaller than, say, 50% of a representative "yield stress" in the polymer (as determined from a uniaxial test).

Another assumption used in our formulation is that the film is inextensible. Such strains, however, may become important when the adhesion of the film is strong. In order to determine whether axial strains are indeed important we suggest the following simple procedure. An average axial stress in a peel test can be defined as $\sigma_a = P/h$. Using the uniaxial stress-strain curve of the material (at an appropriate strain rate) one can then estimate the corresponding axial elastic strain. Furthermore, using σ_a one can also estimate the corresponding creep strain during the test. If the axial strains are indeed smaller than the bending strains, as determined by our analysis, then γ can be determined using Figure 7, together with equation (4.1) above.

When the axial strains are of the same order as the bending strains, however, one needs to modify the kinematic assumption (2.2.6). The strain distribution on a cross-section along the film can be now written as

$$\epsilon(s,z) = -K(s)z + \epsilon_a(s). \tag{4.2}$$

where $\epsilon_a(s)$ is the axial strain, which is an extra unknown to the problem. In such a case, the velocity of crack propagation v_c is, in general, different from the speed of peeling v^∞, and it can be readily shown that

$$v_c = \frac{v^\infty}{1+\epsilon_a^\infty}, \tag{4.3}$$

where ϵ_a^∞ is the axial strain at the end of the unattached part of the film where the peel force is applied. Furthermore, the velocity of material points along the axis of the film varies with the local axial strain as

$$v(s) = \frac{1+\epsilon_a(s)}{1+\epsilon_a^\infty} v^\infty. \tag{4.4}$$

Equations (2.2.8) and (2.2.9) are then no longer valid and the governing equations consist of two coupled integro-differential equations for $K(s)$ and $\epsilon_a(s)$ which need to be solved simultaneously.

We conclude the paper by mentioning that our analysis provides a first step towards a sound understanding of polymer peeling. The effects of non-linear viscoelasticity, residual stress, as well as axial strains are definitely worth studying and will be addressed in detail in a future publication.

Acknowledgment

The authors acknowledge the support of NSF (Grant No. MSM-8657860) and IBM East Fishkill (Grant No. PO 7E 206144 Z).

References

1. G. J. Spies, *J. Aircraft Eng.* **25,** 64 (1953).
2. J. J. Bikerman, *J. Appl. Phys.* **28,** 1484 (1957).
3. D. H. Kaeble, *Trans. Soc. Rheol.* **3,** 161 (1959).

4. D. H. Kaeble, *Trans. Soc. Rheol.*, **4,** 45 (1960).
5. C. Jouwersma, *J. Polymer Sci.* **45,** 253 (1960).
6. J. L. Gardon, *J. Appl. Polymer Sci.* **7,** 643 (1963).
7. A. N. Gent and G. R. Hamed, *J. Adhesion* **7,** 91 (1975).
8. D. W. Nicholson, *Int. J. Fracture* **13,** 279 (1977).
9. F. S. C. Chang, *Trans. Soc. Rheol.* **4,** 75 (1960).
10. K. Kendall, *J. Adhesion* **5,** 105 (1973).
11. N. Aravas, K.-S. Kim and M. J. Loukis, *Material Science and Engineering* **A107,** 159 (1989).
12. W. N. Findley, J. S. Lai and K. Onaran, (North Holland Publishing Company, 1976).
13. B. Harper, private communication.
14. K.-S. Kim, *University of Illinois at Urbana-Champaign, Department of Theoretical and Applied Mechanics, Report No. 472* (March 1985).
15. M. J. Loukis and N. Aravas, "The effects of residual stresses in the peeling of metal films," *IBM Progress Report No. 5* (March 1990).